

Defect Depth Detectability in Austenitic Stainless Steel by Lock in Thermography

by M.Menaka*, D.Sharath *, B.Venkatraman* and Baldev Raj***

* Indira Gandhi Centre for Atomic Research, Kalpakkam-603102, India, bvenkat@igcar.gov.in

***PSG Institutions, PSG College of Technology Campus, Peelamedu, Coimbatore, India, dr.baldev@psg.org.in

Abstract

In this paper, we explore the defect evaluation in austenitic stainless steel using lock in technique and the effect of modulation frequency on the defect detectability in stainless steel. The simulation studies has also been carried out and compared with experimental values. A review of international literature indicates that while such studies have been attempted on materials like Perspex and composites, studies on austenitic stainless steel like AISI 316 have been limited. Austenitic stainless steels are widely used in the nuclear and other process industries. The principal structural materials for the 500 MWe Fast Breeder Reactor being built at Kalpakkam, India is austenitic Stainless Steel type 316LN and 304LN.

1. Introduction

During the last two decades, a number of developments have taken place in the field of thermography. There have been rapid advances in the technology as well as in the techniques of thermography. Technologically, we have excellent IR imaging systems with high frame rates, better detectors with low noise equivalent temperature difference and advanced softwares for enhanced feature detection and evaluation. In the area of techniques in thermography, a number of alternatives have emerged especially in active thermography such as vibrothermography, pulsed thermography, pulse phase thermography etc. A detailed review of the theory, principles and applications can be found in references [1-4].

Lock in Thermography (LT) is an advanced NDE technique, where the inspecting object is heated using a modulated light source which results in periodic variation in surface temperature. The interfaces, like defect, reflects the thermal waves causing interferences of thermal wave which results in change in amplitude and phase of resultant thermal wave. Pioneered by G.Busse [5], this technique has been successfully applied for over a decade for the detection of local heat sources in electronic components, shunt detection in solar cells, NDE of aircraft structures and coating characterisation [6-10]. In this technique, a sinusoidal intensity modulated thermal excitation is used for the detection of subsurface features. The main advantage of lock-in is ability to qualify the depth of the defect with proper calibration.

In this paper, we explore the possibility of using lock-in thermography to quantitatively estimate the depth of the defect from surface, in stainless steel AISI type 316. A review of international literature indicates that while such studies have been attempted on materials like Perspex and composites, studies on austenitic stainless steel like AISI 316 have been very limited [11]. This steel of prime importance in the nuclear industry and is the major structural material for the currently operating and planned Fast Breeder Reactors all over the world in view of its adequate high temperature mechanical properties, compatibility with liquid sodium coolant and good weld ability. This material is also widely used in other industries such as chemical and petrochemical as a structural material due to its high corrosion resistance.

1. Theory

In LT, a modulated light source is used to heat the object. The surface temperature of the object oscillates, with the frequency same as light source, which is monitored using an IR camera. Highly damping thermal waves, generated at front surface, propagates to back surface. When they encounter the interfaces like, defect, they will reflect back and interference will occur between incoming and reflected thermal waves causing change in phase and amplitude of resultant thermal wave. This change in amplitude and phase is calculated at each pixel, using Four Point Correlation method, to get amplitude and phase image [12,13]. Phase image gives better depth information and independent of surface variations when compared to amplitude image [14].

3. Study Approach

Material: AISI type 316 L SS plate of dimension 150 mm (length) x 100 mm (breadth) x 3.54 mm (thickness) was chosen and defects of various size (10 mm, 8 mm, 6 mm, 4 mm and 2 mm) at different depths (0.4 mm, 1.13 mm, 1.78 mm, 2.48 mm, 3.17 mm and 3.36 mm) were then machined using Electro Discharge Machining (EDM). The schematic diagram of the sample is shown in fig. 1.

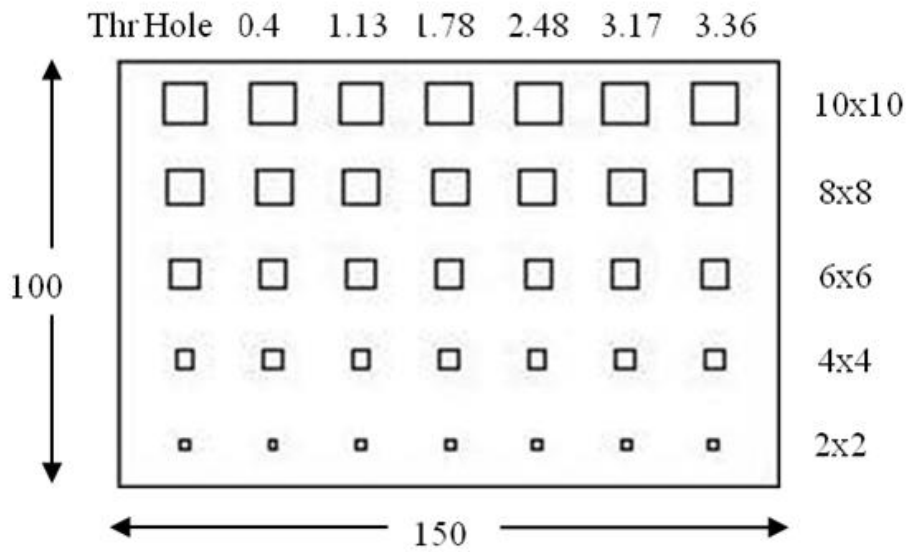


Figure 1: Schematic diagram of the sample

Experimental Set Up: SILVER 420 IR camera (CEDIP) was used for the study which has Indium Antimonide semiconductor detector with 320 x 256 elements which detects IR radiation in the band 3.6 μm – 5.1 μm . The stirling cooling system gives thermal resolution of 25 mK and maximum achievable frame rate is 176 Hz. For LT, two halogen lamps of power 1000 Watts were used as source of heat which was controlled using an amplifier and function generator. ALTAIR software was used for acquiring thermal images while ALTIR LI software was used for lock in analysis. The camera to object distance was kept at 35 cm and lamp to object distance was kept at 40 cm. The schematic diagram of the experimental set up is shown in fig. 2.

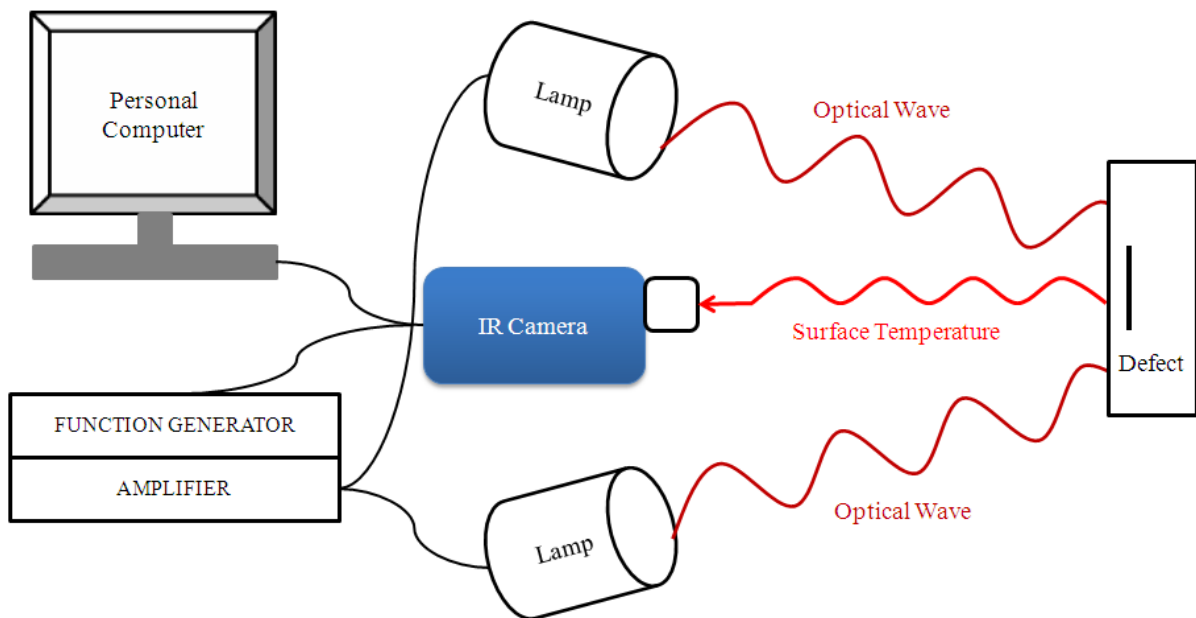


Figure 2: Schematic diagram of LT experimental setup

3.0 Results and Discussion

In general phase contrast method and blind frequency method are widely used for depth quantification in lock-in thermography. In this paper the authors have adopted these two methods for depth evaluation in austenitic steels.

Blind Frequency Method: In Pulsed Phase Thermography (PPT), blind frequency is widely used for depth quantification [15,16]. The thermal diffusion length measured at the blind frequency is the function of defect depth [17]. The relationship between defect depth and blind frequency is given by the following equation,

$$L = C \sqrt{\frac{\alpha}{\pi f_b}} \quad (1)$$

where C is proportionality constant, f_b is the blind frequency for defect of depth L.

The value of C for composite materials using PPT and lock-in thermography has been reported in literature [15,18]. For AISI type 316 L, the value of C was calculated based on theoretical analysis carried out using Bennett and Patty (BP) model [19].

BP model was originally proposed for the photoacoustic methods. LT and photoacoustic method work on the same principle, but the way the output is detected is different. In LT, the modulated light source causes periodic variation in surface temperature which is measured using IR camera and FPC is performed to get the amplitude and phase information. In photoacoustic method, the photoacoustic cell is attached to the surface of the sample which is exposed to modulated light source that causes periodic variation in surface temperature. The temperature changes pressure in the photoacoustic cell which results in generation of acoustic signals which are detected and used for analysis. If the sample is thermally thin, then thermal waves will undergo interference causing change in amplitude and phase angle measurement. The change in phase angle of thermally thin sample and reference sample, which is assumed to be thermally thick, is given by the following equation,

$$\Delta\phi = \tan^{-1} \left\{ \frac{-R_b(1+R_g)\exp(-2a_s L)\sin(2a_s L)}{1-R_g[R_b \exp(-2a_s L)]^2 + R_b(1-R_g)\cos 2a_s L} \right\} \quad (2)$$

where R_b and R_g are the reflection coefficients of sample-backing material interface and sample-gas interface respectively. $a_s L$ is the thermal thickness of the material where a_s is the inverse of thermal diffusion length ($a_s = 1/\mu$). Equation 2 could be used for theoretical analysis of LT, since the equation deals with the thermal wave propagation inside the material, which is same in case of LT and photoacoustic method. In LT, there is no backing material, hence the sample-air interface can be considered as the sample- backing material interface, which is also true for gas-sample interface (front side).

The analysis was done for defects at depths 0.4 mm, 1.13 mm, 1.78 mm and 2.48 mm. The variation of phase angle difference as a function of frequency is shown in fig. 3 (a). The plot shows that the near surface defects have higher blind frequency when compared to deeper defects. The blind frequency was measured for each defect and thermal diffusion length at blind frequency was calculated. According eqn. 1, the plot of defect depth and corresponding diffusion length at blind frequency should be a straight line, passing through the origin with slope C. To obtain the constant C, defect depth is plotted as a function of thermal diffusion length at blind frequency. Then a linear fit is carried out on the data as shown in fig. 3 (b). The analysis showed that the linear fit matches the analytical result with $R^2 = 1$ and slope = $C = 1.57$.

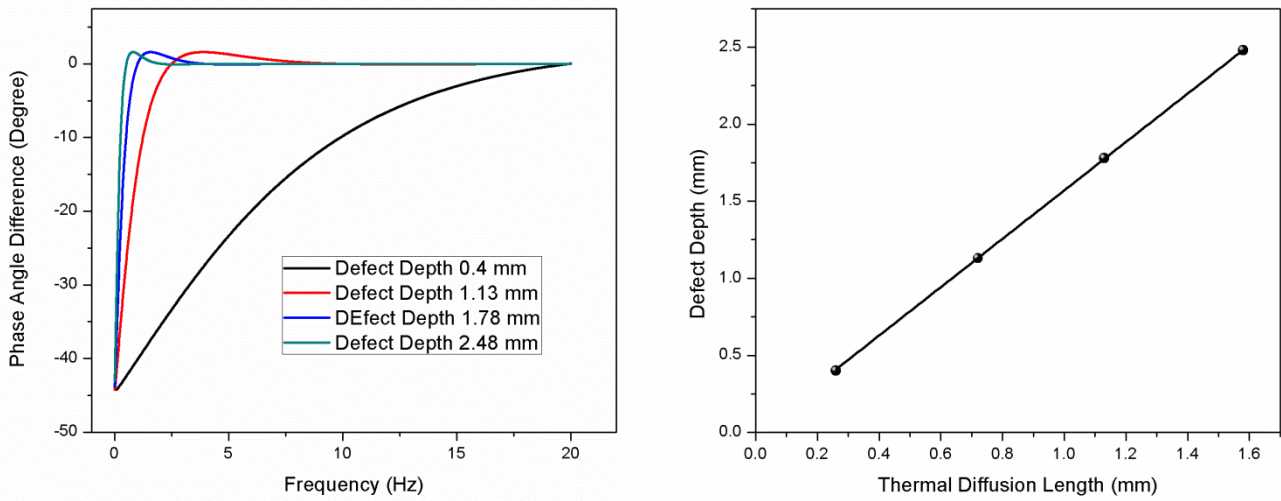


Figure 3: (a) Plot of phase angle difference variation as a function of frequency obtained from Benett Patty model for defects of various depths (b) Defect depth variation as a function of thermal diffusion length at blind frequency

Since LT experiment consumes time, the experiment was initially carried out over a frequency range 0.01 to 0.7 Hz with a frequency step of 0.1 Hz. Then the phase contrast value was computed for defects of size 10 mm x 10 mm at various depths and plotted as a function of frequency (fig. 4). The experiment was conducted at that frequency range with frequency step 0.02 Hz for defects of various depths at the point of phase inversion and the phase contrast value computed and plotted as a function frequency. It was observed that polynomial of order 3 gives better fit to the curve as shown in fig. 5. The blind frequencies were then measured for defects at various depths, thermal diffusion length at the blind frequency computed and the defect depth plotted as a function of diffusion length (fig. 6 (a)). From fig. 6a it can be observed that though it follows the straight line trend, it does not pass through origin, as expected from theoretical analysis. The value of C is computed for each defect depth and a plot of C as a function of defect depth and is shown in fig. 6 (b). From fig. 6 (b), it is observed that C is not a constant as concluded from theoretical analysis, but is a function of defect depth also. The value of C is lower than the expected value 1.57. The comparison between theoretical blind frequency and experimental blind frequency shows that theoretical value is higher than the experimental value.

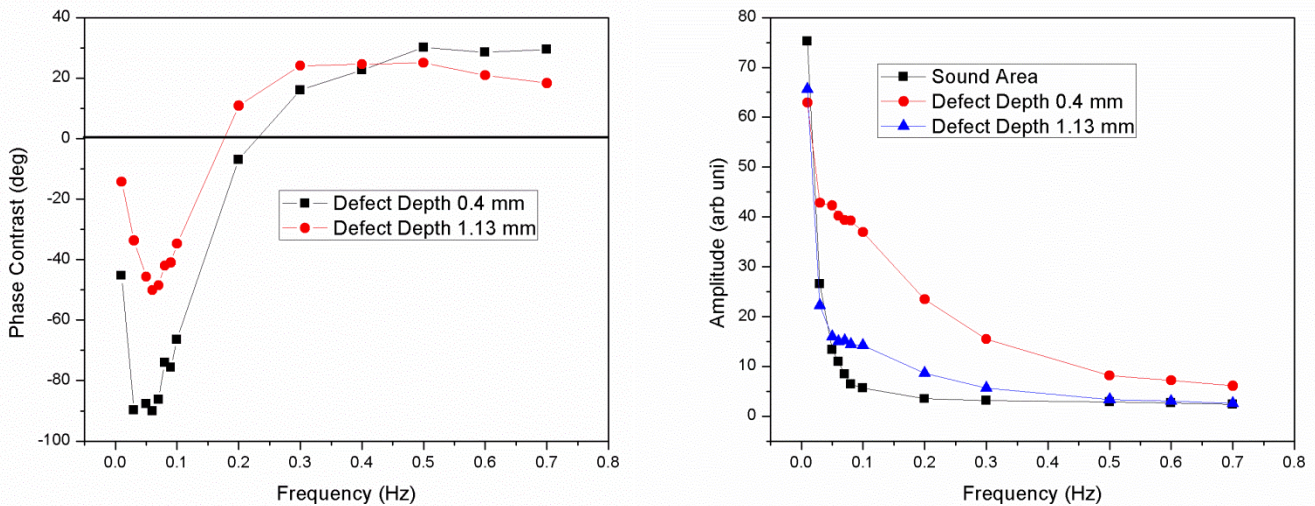


Figure 4: Phase contrast and amplitude variation as a function of frequency

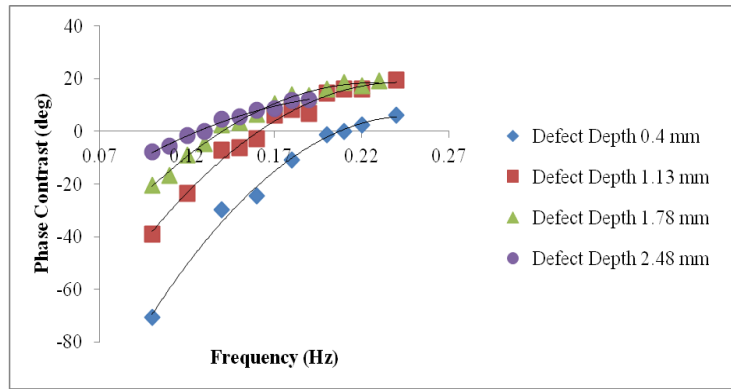


Figure 5: Phase contrast variation as a function of frequency (Experimental)

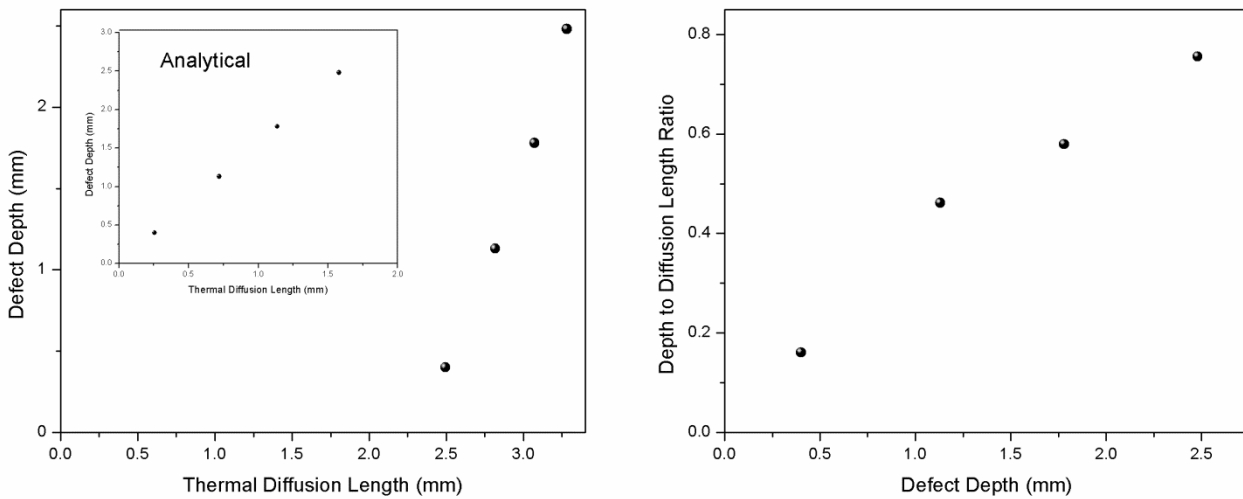


Figure 6: (a) Defect depth vs thermal diffusion length at blind frequency (b) Depth to diffusion length ratio (C) as function of defect depth

To explain the deviation from theoretical prediction, we have considered effect of defect size and shape on blind frequency. The phase contrast was computed for defects of size 10 mm x 10 mm, 8 mm x 8 mm, 6 mm x 6 mm and 4 mm x 4 mm located at a depth of 0.4 mm and plotted as a function of frequency as shown in fig.7(a). From fig.7(a), it can be observed that blind frequency increases as defect size decreases and smaller defect has more effect on blind frequency than the larger defect. This is clearly seen in fig.7(b), which is the plot of variation of blind frequency as a function of defect size. The experiment was repeated with the same parameters as used in the earlier experiment for defects of different shape (circular, square and rectangular). Then the blind frequency was computed for defects of different shape at depth 0.4 mm and is shown in fig.8. From the figure, it can be observed that rectangular shaped defect has greater influence on blind frequency while circular and square shaped defects have comparable blind frequencies. Hence the blind frequency is not only a function of defect depth but also a function of defect size and shape.

The theoretical analysis is a one dimensional approach, where as in the actual case thermal waves follow three dimensional heat flows. This causes the low value of experimental blind frequency when compared to theoretical value. Another source of error is the choice of reference material. In theoretical analysis, the reference is thermally thick (semi infinite material) but it is not true in case of experiment, the reference area chosen in experiment has finite thickness. This also contributes to the deviation in the blind frequency measurement. The theoretical analysis does not account for the effect of defect size and shape which influences the blind frequency to a greater extent. Hence blind frequency cannot be considered as an accurate method for depth quantification.

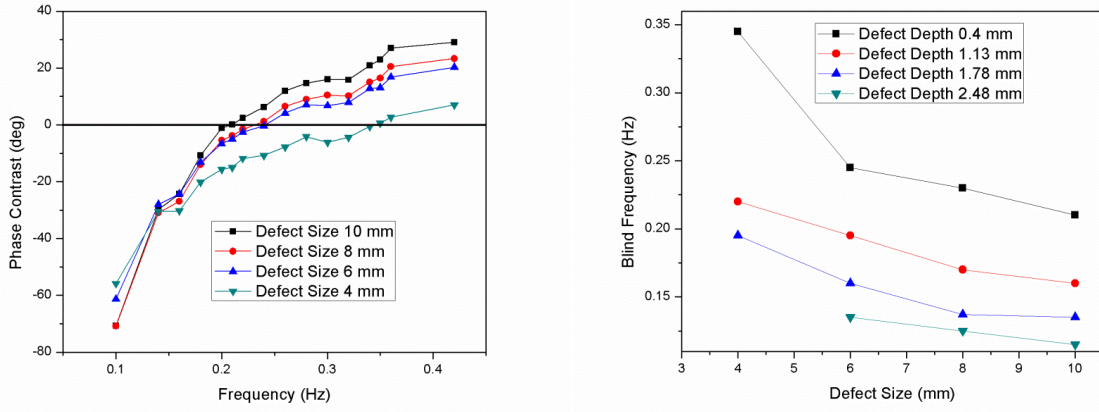


Figure 7: (a) Variation of phase contrast as a function of frequency for defects of various sizes (b) Variation of blind frequency as a function of defect size

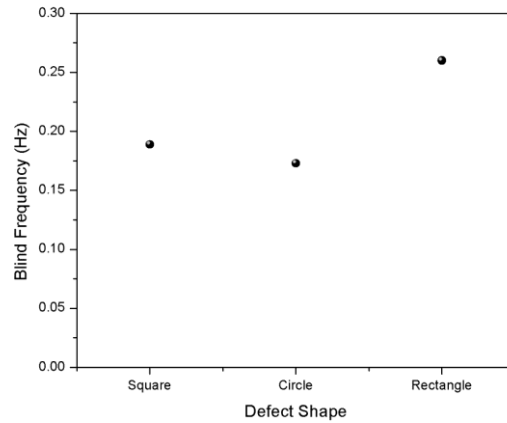


Figure 8: Variation of blind frequency for defects of shape square, circular and rectangle

Phase Contrast Method: An alternate approach proposed for depth quantification is the phase contrast method [20]. Phase contrast decreases as defect depth increases. This is because, as thermal waves from deeper defect reaches the surface, they are highly damped resulting in a weak signal causing lower phase shift when compared to near surface defects. Hence phase contrast could be used as a measure of defect depth. Phase image at optimum frequency was considered for analysis (0.07 Hz), since at optimum frequency phase contrast is maximum and maximum number of defects is detected.

The phase contrast was computed by taking the average phase angle over a defective area and an adjacent non defective area. A rectangle area was selected and the pixel values were averaged over the area to reduce the fluctuation. Since we are working on single frequency, absolute phase contrast was considered. Figure 9 is a plot of defect depth vs phase contrast. It can be observed that the curve is non-linear A polynomial of order 3 (eqn. 3) was observed to gives best fit with $R^2 = 0.998$

$$L = 0.0002(\Delta\phi)^2 + 0.049\phi + 3.01 \quad (3)$$

This is used as calibration plot. The intercept of the fit gives the phase angle value of sound area. To evaluate the efficiency of the above generated calibration plot, the experiment was conducted on another square defect sample under identical experimental conditions. Phase contrast was measured for defects of size 10 mm at various depths (unknown) and the depth was estimated using eqn. 6. The actual depth, predicted depth and the error is given in table 1. From the table we can observe that the error percentage involved in measurement is minimum (less than 10 %).

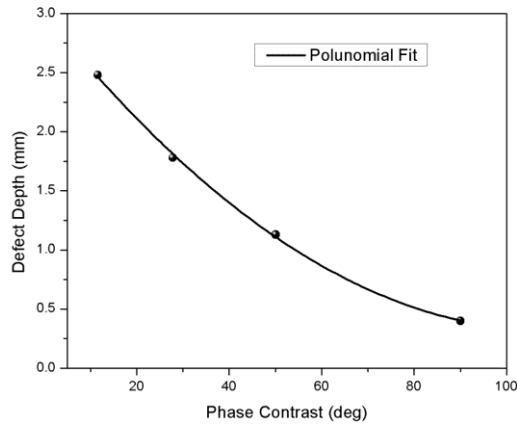


Figure 9: Plot of defect depth vs phase contrast with polynomial fit of order 3

Actual Depth (mm)	Predicted Depth (mm)	% Error
0.5	0.45	10
1.15	1.23	6.9
1.83	1.99	8.7

Table 1: Depth prediction using phase contrast method and error associated with it

4.0 Conclusions:

The present work clearly indicates the ability of LT for defect detection and depth quantification in AISI type 316 L Stainless Steel. Two methods for depth quantification are discussed namely, blind frequency method and phase contrast method. In blind frequency method, thermal diffusion length at blind frequency is proportional to defect depth. To calculate proportionality constant, 1 D analytical modeling was carried out, proposed by Bennett and Patty. The proportionality constant was found to be 1.57 for Stainless Steel system. The experimental investigation showed that the actual value of C is not constant but is a function of defect depth and experimental values are not in agreement with theoretical analysis. To explain this deviation, the effect of defect size and shape on blind frequency was carried out and observed that blind frequency strongly depends on defect size and shape and is not a function of depth alone, which has not been considered in theoretical analysis. Apart from this, theoretical analysis is one dimensional approach, where as the actual case is three dimensional. Hence blind frequency method cannot be used for depth quantification unless a normalization parameter is used. In phase contrast method, the phase angle difference between defective and sound area was computed and used for depth quantification. The calibration plot was generated and used for depth prediction and it was observed that the error associated with measurement was minimum.

REFERENCES

- [1] Xavier P.V.Maldague, Non-Destructive Evaluation of Materials by Infrared Thermography, Springer Verlag, 1993, pp. 45.
- [2] Baldev Raj, B. Venkataraman and C. Babu Rao, " An Overview of Non-Destructive Test Application in Thermography", Journal of NDE, Sept. 1992, pp 1-13.
- [3] B.Venkataraman, Ph.D Dissertation, 2004 University of Madras,
- [4] B.Venkataraman, Baldev Raj and C.K.Mukhophadyay, Characterisation of Tensile Deformation through IR Imaging Technique, Korean J. of NDT, Vol. 22, No. 6, Dec. 2002, pp. 609-620.

- [5] G. Busse, D. Wu, and W. Karpen, Thermal wave imaging with phase sensitive modulated thermography, *J- Appl. Phys.* 71, 1992, pp. 3962-3965.
- [6] J. Rantala, D. Wu, and G. Busse, Amplitude modulated lockin vibrothermography for NDE of polymers and composites, *Research in Nondestructive Evaluation* 7, 1996, pp. 215.
- [7] O. Breitenstein, J. P. Rakotoniaina, M. Kaes, S. Seren, T. Pernau, G. Hahn, W. Warta, J. Isenberg, "Lock-In thermography - a universal tool for local analysis of solar cells", *Proceedings 20th European Photovoltaic Solar Energy Conference*, Barcelona, 2005, pp 590-593.
- [8] Thomas Zweschper, Alexander Dillenz and Gerd Busse, NDE of Adhesive Joints and Riveted Structures with Lock-in Thermography Methods, *Proceedings of SPIE, the International Society for Optical Engineering*, 2001, Vol. 4360, pp. 567-573 .
- [9] W.Bai and B.S.Wong, Evaluation of Defects in Composite Plates under Convective Environments using Lock-in Thermography, *Measurement Science and Technology*, Vol. 12, pp. 142-150.
- [10] B.Venkatraman, M.Menaka, R.Subbaratnam and Baldev Raj, Characterisation of Colmonoy Coatings using Lock-in Thermography, *Proceedings 17th World Conference on Nondestructive Testing in CD-ROM*, 25-28 Oct 2008, Shanghai, China
- [11] C.Wallbrink, S.A. Wade and R.Jones, The effect of size on the quantitative estimation of defect depth in steel structures using lock-in thermography, *Journal of applied physics*, 101(2007) 104907.
- [12] G. Busse, D. Wu, W. Karpen, Thermal wave imaging with phase sensitive modulated thermography, *Journal of Applied Physics*, 71 (1992) 3962-3965
- [13] Darryl Almond and Pravin Patel, *Photothermal science and techniques*, Chapman & Hall, London (1996)
- [14] G. Busse, Optoacoustic phase angle measurement for probing a metal, *Applied Physics Letters*, 35 (1979) 759-760
- [15] C. Ibarra-Castanedo, X. Maldague, Defect depth retrieval from pulsed phase thermographic data on Plexiglas and Aluminum samples, *Proceedings of SPIE, Thermosense XXVI*, 5405 (2004) 348-355
- [16] Clemente Ibarra-Castanedo, Xavier P. V. Maldague, Interactive methodology for optimized defect characterization by quantitative pulsed phase thermography, *Research in Non Destructive Evaluation*, 16 (2005) 175-193
- [17] G. Giorleo, C. Meola, A. Squillace, Analysis of defective carbon epoxy by means of Lock-in thermography, *Research in Nondestructive Evaluation*, 12 (2000) 241-250
- [18] C. Zoecke, A. Langmeier, W. Arnold, Size retrieval of defects in composite material with lock-in thermography, *15th International Conference on Photoacoustic and Photothermal Phenomena (ICPPP15)*, *Journal of Physics: Conference Series* 214 (2010) 012093
- [19] C. A. Bennett Jr., R. R. Patty, Thermal wave interferometry: A potential application of the photoacoustic effect, *Applied Optics*, 21 (1982) 49-54
- [20] M. Menaka, D. Sharath, B. Venkatraman and Baldev Raj, Precise depth detection of EDM notches by lock-in thermography, *Journal of Non destructive Testing and Evaluation*, 8 (2009), 15-18